



Review

On the electrostatics of DNA in chromatin

Klemen Bohinc^{1,*} and Leo Lue²

¹ Faculty of Health Sciences, University of Ljubljana, Zdravstvena 5, SI-1000 Ljubljana, Slovenia

² Department of Chemical and Process Engineering, University of Strathclyde, James Weir Building, 75 Montrose Street, Glasgow G1 1XJ, UK

* **Correspondence:** Email: klemen.bohinc@zf.uni-lj.si; Tel: +386-1-300-11-70;
Fax: +386-1-300-11-19.

Abstract: We examine the interaction between DNA molecules immersed in an aqueous solution of oppositely charged, trivalent spermidine molecules. The DNA molecules are modeled as planar, like-charged surfaces immersed in an aqueous solution of multivalent, rod-like ions consisting of rigidly bonded point charges. An approximate field theory is used to determine the properties of this system from the weak to the intermediate through to the strong coupling regimes. In the weak coupling limit, the interaction between the charged surfaces is only repulsive, whereas in the intermediate coupling regime, the rod-like ions with spatial charge distribution can induce attractive force between the charged surfaces. In the strong coupling limit, the inter-ionic charge correlations induce attractive interaction at short separations between the surfaces. This theoretical study can give new insights in the problem of interaction between DNA molecules mediated by trivalent spermidine molecules.

Keywords: electrostatics; field theory; DNA; multivalent ions; chromatin

1. Introduction

The nucleus of eukaryotic cells possess chromatin, which is mostly composed of complexes of nuclei acids with proteins. Roughly 80% of DNA within chromatin is present in the form of protein-DNA complexes called nucleosomes. Further, nucleosomes are composed of base pairs of double stranded DNA. The central part of the nucleosome is the nucleosome core particle which consists of 146-147 base pairs of DNA wrapped as a superhelix around histones. A variable length of DNA connects nucleosome core particles [1].

For better understanding of interactions between charged structures within the nucleosome more insight into the interaction between DNA molecules induced by multivalent ions is needed. In vitro, DNA compaction can be induced by the addition of multivalent counterions [2, 3]. Positively charged

colloidal particles [4, 6] and zwitterionic lipids [7, 8] form complexes with DNA.

In the absence of counterions, similarly charged macroions or molecules repel each other. The presence of multivalent counterions, however, can lead to an intuitively surprising effective attractive interaction between similarly charged particles in aqueous solution. Here we mention a few examples. The attraction can be mediated by the correlated motion of mobile multivalent ions in the aqueous solution [9]. Hexagonal arrays of double stranded (ds) DNA can be induced by the presence of polyamines and at least three-valent ions; some divalent ions, like manganese and cadmium, can even lead to the formation of DNA arrays [3]. Divalent diamine ions can induce aggregation of rod-like M13 viruses [10]. Divalent barium ions can mediate network formation in actin solutions [11]. Divalent ions can also induce adsorption of DNA onto zwitterionic lipid layers [12]. Multivalent ions with spatially distributed charges show a strong tendency to aggregate like-charged macroions. Here we mention positively charged colloids that condense DNA [6] and DNA that induces attractive interaction between cationic lipid membranes [4].

DNA condensation is related to the process of compacting DNA [3], which is important to its function in gene regulation. Condensed DNA has extraordinary properties and has often been used as a model system in physics and biology [6]. In eucaryotic cells, DNA typically has a length of a few centimeters; after packing the size should be few microns in order to enter the nucleus. In dinoflagellates, we can distinguish liquid-crystalline chromosomal ordering [5], fully being without or with a smaller complement of histone proteins. In other cases, DNA is organized in the cell nucleus with the help of histones. Here, the basic unit of DNA compaction is the nucleosome. In the nucleosome the double helix is wrapped around a histone octamer containing two copies of each of the histones H2A, H2B, H3 and H4.

DNA between nucleosomes can be bound by the linker histone H1. They facilitate the packaging of the beads on the string, with a size of around 10 nm. nucleosomal chain into a more condensed fiber. Its size is around 30nm. During cell division, chromatin is optimized to allow easy access of transcription factors to active genes. These genes are characterized by a less compact structure called euchromatin, and to facilitate protein access in very tightly packed regions (heterochromatin). In the process of cell division, chromatin compacts even further to form chromosomes, which come into contact with the large mechanical interaction that drag them into each of the two daughter cells [3].

In many situations, the interactions between DNA complexes are dominated by electrostatic interactions. In addition, the relevant separation distances and the sizes of the mobile ions in solution are usually much smaller the dimensions of these complexes. Consequently, a popular simplified description of DNA molecules or complexes has been to treat them as uniformly charged surfaces, in order to gain insight into their behavior.

There are many theoretical studies on the interaction between charged surfaces. The classical Poisson-Boltzmann (PB) theory [13, 14] predicts only repulsive interaction [9]. Hence, the attractive interaction must be caused by the effects beyond those captured by classical PB theory, such as charge-charge correlations [15, 16]. Indeed, accounting for inter-ionic correlations between multivalent counterions and charged surfaces leads to the possibility of attractive interaction between like-charged surfaces [17, 18]. The presence of an attractive interaction between two like-charged surfaces immersed in an aqueous solution composed of divalent ions in the limit of high surface charge density was first calculated by Monte-Carlo (MC) simulations of Guldbbrand et al. [19]. After Guldbbrand, more detailed MC simulations [15, 20, 21] showed that attractive interactions between equally charged

surfaces may arise for high surface charge density, low temperature, low relative permittivity and multivalent counterions.

While mean-field theories are able to describe the interaction between weakly charged surfaces, they breakdown as the surface charge densities increase. The mean field approximation can be systematically improved by including fluctuations around the saddle point. Coalson and Duncan utilized a lattice field theory approach to calculate the first order corrections to the mean-field approximation for the free energy of a system of fixed charged macroions surrounded by mobile ions [22]. The lattice field theory approach was later generalized to include the finite size of the simple mobile ions [23], mobile dipoles and charged polymer chains [24, 25].

Rather than being point-like, ions usually have an internal structure with individually separated charges and additional internal degrees of freedom. Examples include polyamines (e.g., diamines, spermidines, spermines), which can be described as rod-like ions composed of individual point charges that are spatially well separated from each other. Many biologically important ligands can be considered as rod-like particles with two individual point-charges separated by a fixed distance. The rod-like approximation could be relevant not only for small counterions, but also, as a first-order approximation to proteins that bridge between DNA molecules, (e.g. H-NS and HU in bacteria), although these interactions are at least partially sequence-specific (Navarre et al., 2006 [26]). The separation between the individual charges are, in general, not small compared with the electrostatic screening length typically in solution.

Bohinc et al. [27, 28, 29, 30] showed that intra-ionic correlations induced by the bonds within a particular rod-like ion are enough to change repulsive into attractive interactions between like-charged surfaces. The minimum of the free energy appears when the rod-like ions are oriented perpendicularly to the like-charged surfaces, thus connecting them [31]. The rod-like ions bridge the two surfaces, resulting in the attraction [3]. These theoretical predictions were confirmed by Monte Carlo simulations [32, 28, 30, 33]. These systems was later examined in the intermediate and strong coupling regimes, where the interionic correlations between the charges alone can lead to an attraction between the like-charged surfaces [34]. The theory was generalized to systems with polydisperse rod lengths and arbitrary charge distributions along the rods [35, 36]. The addition of monovalent point-like salt ions can turn the attraction between the plates to a repulsive interaction due to screening [30]. The hydration shell around the ions with spatially extended charge was introduced. The first attempt has been made by introducing spheroidal ions with two charges embedded in a spherical structure [37, 38]. The model has been extended to ions with a smooth charge distribution on the spherical surface [39] and to uranyl ions [40].

In the past, many experimental studies on DNA were made. In the 1970s, the first in vitro experiments were performed [41, 42]. In the experiments, DNA is compacted by adding different condensing agents, which simple inorganic ions or large macromolecules. DNA compaction is an important model systems to elucidate DNA's function in vivo and also to achieve controlled drug delivery in gene therapy. In the last 45 years of experiments, DNA condensation has been studied using a wide variety of different methods, such as sedimentation [43], light scattering [44], viscometry [45, 46], osmotic equilibrium [47, 48], IR, UV and Raman spectroscopy [49], electron microscopy [50], and atomic force microscopy [51]. More recently, capillary electrophoresis techniques [52] and single-molecule optical and magnetic tweezers [53, 54, 55, 56] have been used.

In this review, we examine the interaction between two like-charged macromolecules (e.g., DNAs)

represented by charged planar surfaces embedded in a solution of trivalent rod-like ions (e.g., spermidine molecules). The only interactions between the rod-like counterions are the electrostatic interactions. We consider the conditions for attractive interactions mediated by multivalent rod-like ions and examine the appearance of attractive interactions between like-charged surfaces due to the internal structure of multivalent ions, as well as to the correlations between different ions. The description is based on a general field theoretic method, modified to include ions with a spatially distributed charge confined between large, highly charged macroions in a planar geometry.

2. Theory

We simplify our system (Fig. 1) to two infinitely large planar surfaces separated by a distance D . The plates have a surface charge density Σ and are embedded in an aqueous solution of rod-like ions. The ions consist of three linearly bonded point charges of magnitude q . Ions often dissociate and become mobile in water, due to its high dielectric constant, $\epsilon \approx 78$, which reduces charge-countercharge attraction, thus favoring the entropic gain that comes with the dissociation process. The competition between electrostatic and thermal energy can be expressed in terms of the Bjerrum length $l_B = q^2/(\epsilon k_B T)$, the distance at which two ions of charge q have an interaction energy of $k_B T$, where k_B is Boltzmann constant, and T is the absolute temperature. In water at room temperature, the Bjerrum length between monovalent ions is 0.7 nm. In addition to the Bjerrum length, a second length scale is the Gouy-Chapman length $\mu = q/(2\pi l_B \Sigma)$. This length characterizes the distance at which the counterion-wall interaction energy equals the thermal energy of the counterion. The Gouy-Chapman length characterizes the thickness of the counterion layer around a charged wall. The third scale length is the distance D between the plates. A key parameter that governs the physics of the system is the coupling parameter [16, 15]

$$\Xi = \frac{l_B}{\mu}, \quad (1)$$

which is the ratio of the Bjerrum and Gouy-Chapman lengths. Roughly expressed, the coupling parameter compares the strength of the interaction between counterions and the interaction between a counterion and a charged surface. In this sense, it quantifies the strength of the electrostatic interactions. Small values of Ξ define the weak coupling regime [57], where the mean-field theory is valid. Large values of Ξ define the strong coupling regime, where charges at the surface are strongly correlated.

The only interaction between the charges in the system are the electrostatic; excluded volume and other specific interactions are neglected. The electrostatic interaction energy E can be expressed as

$$E = \frac{1}{2} \int d\mathbf{r} d\mathbf{r}' Q(\mathbf{r}) G(\mathbf{r}, \mathbf{r}') Q(\mathbf{r}') - \sum_{k=1}^N e^{\text{se}}(\mathbf{R}_k, \hat{\mathbf{n}}_k) \quad (2)$$

where $G(\mathbf{r}, \mathbf{r}') = \epsilon^{-1} |\mathbf{r} - \mathbf{r}'|^{-1}$ is the Green's function of the Poisson equation, which relates how the electric potential propagates from a unit point charge in the system. The charge density $Q(\mathbf{r})$ includes fixed charge densities, such as those on both surfaces, and mobile charges, such as the counterions charges. The final term in Eq. (2) is the self-energy of the dimer e^{se} , which is the interaction energy of the charges with the electric field generated by its own charges; \mathbf{R}_k is the position of trimer k , and $\hat{\mathbf{n}}_k$.

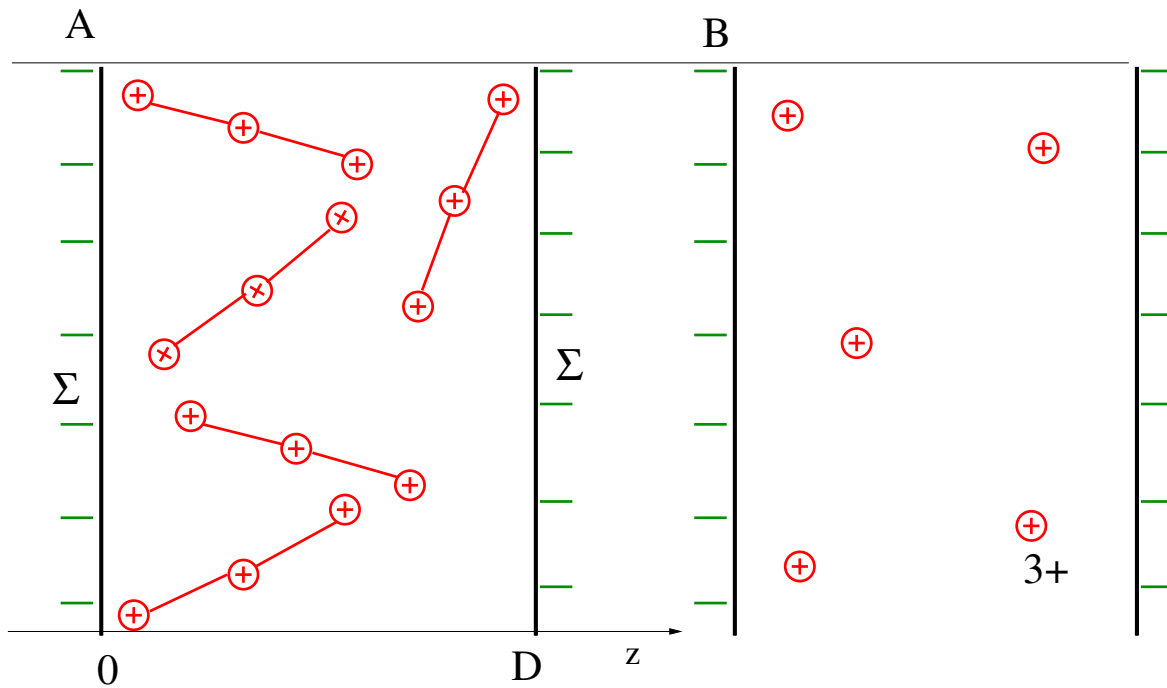


Figure 1. A schematic illustration of two like charged planar macroions embedded in a solution of trivalent rod-like counterions (A) or three-valent point-like counterions (B).

The grand canonical partition function of the system is given an integral over all possible counterion positions and orientations. Using Hubbard-Stratonovich transformation, this integral can be written in terms of a fluctuating field φ , which is related to the electrostatic potential. The integration over the coordinates of the ions is replaced by a functional integral over all possible shapes of the electrostatic potential. This is possible because there is, up to a gauge degree of freedom, a one-to-one correspondence between charge distributions and electrostatic potential. The grand canonical partition function is given by

$$Z_G = \frac{1}{\sqrt{\det G^{-1}}} \int \mathcal{D}\varphi(\cdot) e^{-\beta H[\varphi]/\Xi}, \quad (3)$$

where the Hamiltonian H is

$$H[\varphi] = \frac{1}{2} \int d\mathbf{r} d\mathbf{r}' \varphi(\mathbf{r}) G^{-1}(\mathbf{r}, \mathbf{r}') \varphi(\mathbf{r}') + \int d\mathbf{r} \Sigma(\mathbf{r}) i\varphi(\mathbf{r}) - \frac{\lambda}{\beta} \int d\mathbf{r} e^{-\beta q i \varphi(\mathbf{r})}, \quad (4)$$

where λ is the fugacity of the mobile ions. In the last step, all the quantities were transformed into dimensionless form.

The *weak-coupling limit* occurs for low counterion valency and small surface charge density and corresponds to the case where the coupling parameter $\Xi \ll 1$. The prefactor in front of the field-theoretic action $E[\varphi]$ in the exponent of the grand-canonical partition function is large. Consequently, the contribution of fluctuations of φ around the saddle point value is not significant in the weak coupling limit. The functional integral is dominated by the integrand evaluated at the saddle point φ_0 , which is determined by the equation:

$$\left. \frac{\delta E[\varphi]}{\delta \varphi(\mathbf{r})} \right|_{\varphi_0} = 0. \quad (5)$$

The result is the standard Poisson-Boltzmann theory

$$-\frac{\epsilon}{4\pi}\nabla^2\phi(\mathbf{r}) = q\lambda e^{-\beta q\phi(\mathbf{r})}. \quad (6)$$

where $\phi(\mathbf{r}) = i\varphi_0(\mathbf{r})$ is the mean electrostatic potential in the system.

The *strong coupling limit* corresponds to the case where the coupling parameter $\Xi \rightarrow \infty$, and, therefore, the prefactor in front of the field-theoretic action $E[\varphi]$ in the exponent of the grand-canonical partition function is small. We make a perturbation expansion of the partition function in the fugacity λ . In this case, the ion density is given to first order by

$$\varrho(\mathbf{r}) = \lambda e^{-\beta W_s(\mathbf{r}) - \beta W_{0c}(\mathbf{r})} \quad (7)$$

where the counterion self-energy is $W_s(\mathbf{r}) = \frac{1}{2}q^2 G(\mathbf{r}, \mathbf{r})$, and the wall-counterion interaction is $W_{0c}(\mathbf{r}) = q \int d\mathbf{r}' G(\mathbf{r}, \mathbf{r}') \rho_0(\mathbf{r}')$. The fixed charge density is denoted by $\rho_0(\mathbf{r}')$. In the case of two planar charged surfaces located at $z = 0$ and $z = D$ the fixed charge density becomes $\rho_0(\mathbf{r}') = \Sigma[\delta(z) + \delta(z - D)]$, where $\delta(z)$ is the delta function.

In order to treat systems at intermediate couplings, we divide the the field φ into short wavelength and long wavelength contributions. The functional integration over the long wavelength field is evaluated using the mean field approximation, and the functional integration over the short wavelength field is approximated using a cumulant expansion. The length scale used to distinguish between short and long wavelength fields is chosen so as to make the free energy of the system stationary to first order. The resulting theory reduces to a modified Poisson-Boltzmann theory at weak electrostatic couplings and is accurate from the weak coupling limit through the intermediate coupling regime to the strong coupling limit. Details are described in Refs. [34].

3. Results and Discussion

We present results for the system of trivalent rod-like counterions or trivalent point-like counterions between two like-charged surfaces (see Figs. 1A and B). The length of rod-like counterions is 1 nm, with two elementary charges located at each end of the rod and one elementary charge located at its center. The Bjerrum length is 0.7 nm, because the system is immersed in water. The following description is based on numerical solutions of integro-differential equations presented in the previous section.

In Fig. 2, the equilibrium distance between two like-charged surfaces as a function of surface charge density Σ is shown. The curves corresponds to the conditions at which the pressure between the plates is zero and separate regions where the interaction between the plates is attractive from where it is repulsive. The solid red line corresponds to the case with rod-like trivalent counterions, and the dashed black line corresponds to point trivalent counterions.

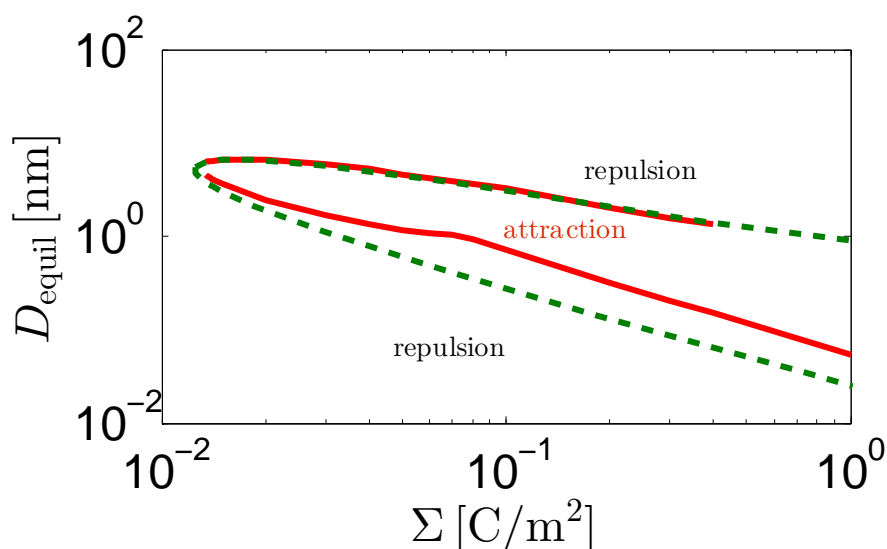


Figure 2. The regions of attractive and repulsive interaction between like charged surfaces. Equilibrium plate separation D_{equil} as a function of the surface charge density for trivalent rod-like counterions (red line) and for trivalent point-like ions (black line). Figure adapted from Ref. [36].

We find that the attraction occurs at larger distances as the surface charge densities of the plates becomes smaller [36, 58]. Increasing the length of the counterions decreases the region of attraction. For the rod-like counterion, there is a cusp in the equilibrium curve at a plate separation of about 1 nm and a plate surface charge density of 0.08 C m^{-2} . This separates the region of attraction into roughly two areas. The region above and to the left of this point corresponds to a bridge mechanism inducing the attraction, where the counterion “connects” the two plates. The region below and to the right of this point corresponds to interionic correlations inducing the attraction.

The pressure as a function of the plate separation is shown in Fig. 3. For a surface charge density $\Sigma = 0.01 \text{ C m}^{-2}$, the interaction between the plates is entirely repulsive, but for $\Sigma = 0.1 \text{ C m}^{-2}$, an attractive interaction between the plates is observed. For small surface charge densities, only repulsive interactions between like charged plates are observed. If the surface charge density or the valency is increased, then an attractive interaction between the plates is obtained. The increased valency decreases the equilibrium distance between the surfaces. The zeroes in the pressure correspond to the extremum (minimum or maximum) in the interaction free energy between. The zero pressure at the separations equal to the length of rods can be associated with the bridging of the rod like particles. The zero in the pressure located at shorter separations is associated with the attraction between plates in the intermediate / strong coupling regime, where the ions are adsorbed to the charged surfaces. The increased valency can switch the bridging to the attractive interactions at short distances between the plates.

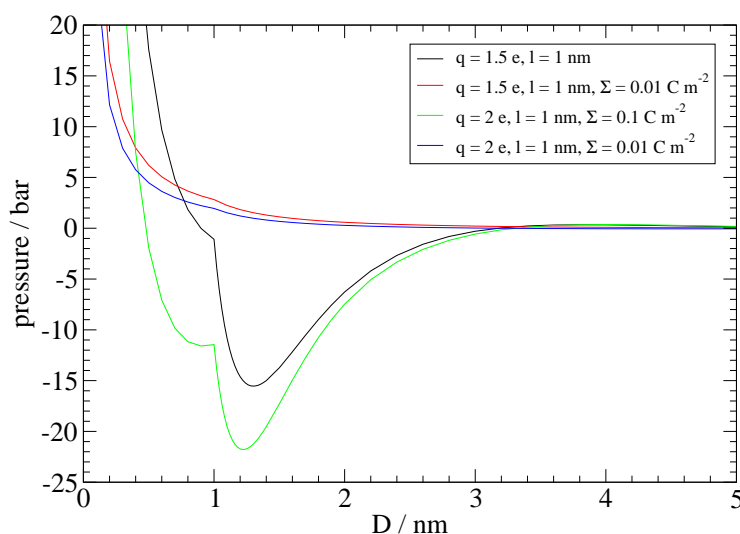


Figure 3. Pressure as a function of the separation between the charged surfaces for rod-like ions of length $l = 1 \text{ nm}$. The surface charge density are $\Sigma = 0.01 \text{ C m}^{-2}$ and $\Sigma = 0.1 \text{ C m}^{-2}$. The dashed lines correspond to valency $Z = 1.5$, and the full lines correspond to valency $Z = 2$.

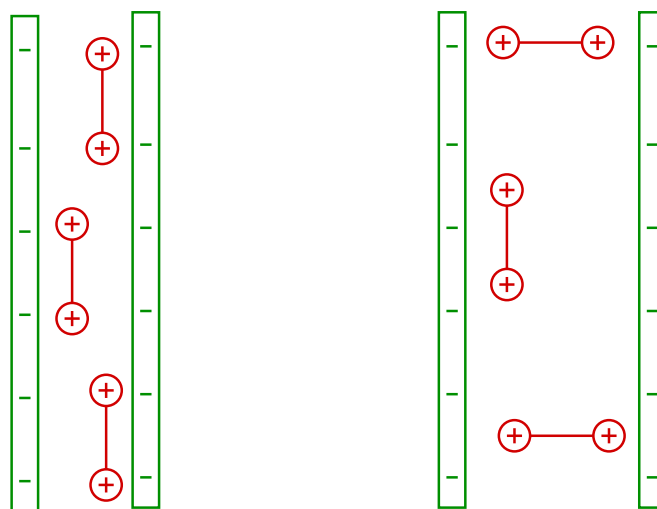


Figure 4. Illustration of DNA-DNA interactions mediated by counterion correlations. (A) DNA-DNA attraction arises due to correlated arrangements of bound ligands. (B) The ions preferentially orient either parallel or perpendicular to the macroion surfaces. Those aligning perpendicular give rise to the bridging effect.

To fully understand DNA-DNA attraction, the correlations between counterions must also be considered. The fact that interionic correlations can lead to attraction was realized early and later studied by Monte-Carlo simulations and various other methods. A simple interpretation of the mechanism that leads to attraction can be given at zero temperature, where counterions condense onto the charged surface. The Coulombic repulsion between condensed counterions produces an alternating pattern of

positive and negative charges on the surface. Two such opposing patterns adjust complementarily to each other and give rise to short-range attractive forces (shown by Grosberg in 2002 [59]).

In the presence of rod-like counterions, the energetically most favorable distance between the charged surfaces of two DNA molecules corresponds to the length of the counterions. At this distance, there are two main orientations of rod-like particles: either oriented in parallel or perpendicular to the charged surfaces (see Fig. 4). Other orientations are less likely. The parallel and perpendicular orientations indicate the tendency for the positive protein charges to be in contact with the negatively charged DNA surface. At high surface charge densities, both orientations are more pronounced. The particles which are perpendicular to the charged surfaces connect the surfaces and act as bridges. This bridging mechanism can lead to attractive interactions between DNA molecules, as confirmed by Monte Carlo simulations. At larger DNA-DNA separations, the rod-like counterions tend to remain adsorbed and parallel to the charged surfaces, and the bridging disappears. At high surface charge densities, interionic charge correlations also contribute [34] and can lead to an attractive interaction between surfacem, even without bridging.

4. Conclusions

In conclusion, we have examined the influence of the charge distribution within a counterion on the interaction between like-charged surfaces, which is a very rough approximation of DNA in chromatin. We have used a previously developed approximate field theory which is known to provide accurate predictions for multivalent ions. The theoretical results are in good agreement with Monte Carlo simulation data, from the weak through to the strong coupling regimes.

Generally, for sufficiently long rod-like counterions, there are two distinct regions of attractions between the plates. One occurs at plate separations that are about the length of the counterion rods, which corresponds to bridging of the counterions across both plates. In addition to bridging, an attractive region occurs at shorter surface separations, which corresponds to correlations between the counterions. With decreasing length of the rod-like counterions, the attractive region associated with “bridging” extends to shorter surface separations.

These theoretical results give new insights for the study of interactions between DNA molecules induced by trivalent rod-like ions, relevant to DNA condensation by addition of spermidine [3]. Clearly, electrostatic interactions are among the most important forces which control chromatin compaction, and their detailed action in epigenetic regulation remains to be explored. In future, this model could be also applicable to the chromatin fibers [60], as well as to the case of DNA linkers between nucleosomes [61].

Conflict of Interest

All authors declare no conflict of interest in this paper.

References

1. Korolev N, Vorontsova OV, Nordenskiöld L (2007) Physicochemical analysis of electrostatic foundation for DNA-protein interactions in chromatin transformations. *Prog Biophys Mol Biol* 95: 23–49.

2. Bloomfield VA (1997) DNA condensation by multivalent cations. *Biopolymers* 44: 269.
3. Teif VB, Bohinc K (2011) Physicochemical analysis of electrostatic foundation for DNA-protein interactions in chromatin transformations. *Prog Biophys Mol Biol* 105: 208–282.
4. Radler JO, Koltover I, Salditt T, et al. (1997) Structure of DNA-cationic liposome complexes: DNA intercalation in multilamellar membranes in distinct interhelical packing regimes. *Science* 275: 810–814.
5. Chow MH, Yan KTH, Bennett MJ, et al. (2010) Birefringence and DNA condensation of liquid crystalline chromosomes. *Eukaryotic Cell* 9:1577-1587.
6. Gelbart WM, Bruinsma RF, Pincus PA, et al. (2000) DNA-inspired electrostatics Physicochemical analysis of electrostatic foundation for DNA-protein interactions in chromatin transformations. *Physics Today* 53:38–44.
7. Mengistu DH, Bohinc K, May S, (2009) Binding of DNA to zwitterionic lipid layers mediated by divalent cations. *J Phys Chem B* 113: 12277–12282.
8. Raedler JO, Koltover I, Salditt T, et al. (1997) Structure of DNA-cationic liposome complexes: DNA intercalation in multilamellar membranes in distinct interhelical packing regimes. *Science* 275: 810–814.
9. Evans DF, Wennerström H (1994) The colloidal domain, where physics, chemistry, biology and technology meet. , 2 Eds., New York: VCH Publishers.
10. Butler JC, Angelini T, Tang JX, et al. (2003) Ion multivalence and like-charge polyelectrolyte attraction. *Phys Rev Lett* 91: 028301.
11. Angelini TE, Liang H, Wriggers W, et al. (2003) Like-charge attraction between polyelectrolytes induced by counterion charge density waves. *Proc Nat Acad Sci U S A* 100: 8634–8637.
12. Bohinc K, Brezesinski G, May S (2012) Modeling the influence of adsorbed DNA on the lateral pressure and tilt transition of a zwitterionic lipid monolayer. *Phys Chem Chem Phys* 40: 10613–10621.
13. Gouy MG (1910) Sur la constitution de la charge électrique à la surface d'un électrolyte. *J Phys Radium (Paris)* 9: 457–468.
14. Chapman DL (1913) A Contribution to the Theory of Electrocapillarity. *Philos Mag* 6: 455–481.
15. Moreira AG, Netz RR (2001) Binding of similarly charged plates with counterions only Modeling the influence of adsorbed DNA on the lateral pressure and tilt transition of a zwitterionic lipid monolayer. *Phys Rev Lett* 87: 078301.
16. Shklovskii BI (1999) Screening of a macroion by multivalent ions: Correlation-induced inversion of charge. *Phys Rev E* 60: 5802–5811.
17. Carnie S, McLaughlin S (1983) Large divalent-cations and electrostatic potentials adjacent to membranes - a theoretical calculation. *Biophys J* 44: 325–332.
18. Kirkwood JG, Shumaker JB (1953) Forces Between Protein Molecules in Solution Arising from Fluctuations in Proton Charge and Configuration. *Proc Nat Acad Sci U S A* 38: 863–871.
19. Gulbrand L, Jönsson B, Wennerström H, et al. (1984) Electrical double layer forces. A Monte Carlo study. *J Chem Phys* 80: 2221–2228.

20. Reščič J, Linse P (2000) Charged colloidal solutions with short flexible counterions. *J Phys Chem B* 32: 7852–7857.
21. Svensson B, Jönsson B (1984) The interaction between charged aggregates in electrolyte solution - a Monte-Carlo simulation study. *Chem Phys Lett* 108: 580–584.
22. Coalson RD, Duncan A (1992) Systematic ionic screening theory of macroions. *J Chem Phys* 97: 5653–5661.
23. Coalson RD, Walsh AM, Duncan A, et al. (1995) Statistical-mechanics of a Coulomb gas with finite-size particles - a lattice field theory. *J Chem Phys* 102: 4584–4594.
24. Tsonchev S, Coalson RD, Duncan A (1999) Statistical mechanics of charged polymers in electrolyte solutions: A lattice field theory approach. *Phys Rev E* 60: 4257–4267.
25. Tsonchev S, Coalson RD, Duncan A (2007) Partitioning of a polymer chain between a confining cavity and a gel. *Phys Rev E* 76: 041804.
26. Navarre WW, Porwollik S, Wang Y, et al. (2006) Selective silencing of foreign DNA with low GC content by the H-NS protein in Salmonella. *Science* 313: 236–238.
27. Bohinc K, Igljč A, May S (2004) Interaction between macroions mediated by divalent rod-like ions. *Europhys Lett* 68: 494–500.
28. May S, Igljč S, Reščič S, et al. (2008) Bridging like-charged macroions through long divalent rodlike ions. *J Phys Chem B* 112: 1685–1692.
29. Maset S, Bohinc K (2007) Orientations of dipoles restricted by two oppositely charged walls. *J Phys A* 40: 11815–11826.
30. Maset S, Reščič J, May S, et al. (2009) Attraction between like-charged surfaces induced by orientational ordering of divalent rigid rod-like counterions: theory and simulations. *J Phys A* 42: 105401.
31. May S, Bohinc K (2014) Mean-field electrostatics of stiff rod-like ions, Eedited by: Dean D, Dobnikar J, Naji A and Podgornik R, *lectrostatics of Soft and Disordered Matter*, 1.st Eds., Pan Stanford Publishing, 335–346.
32. Kim YW, Yi J, Pincus PA (2008) Attractions between Like-Charged Surfaces with Dumbbell-Shaped Counterions. *Phys Rev Lett* 101: 208305.
33. Grime MA, Khan MO, Bohinc K (2010) Interaction between Charged Surfaces Mediated by Rodlike Counterions: The Influence of Discrete Charge Distribution in the Solution and on the Surfaces. *Langmuir* 26: 6343–6349.
34. Hatlo MM, Bohinc K, Lue L (2010) The properties of dimers confined between two charged plates. *J Chem Phys* 132: 114102.
35. Bohinc K, Reščič J, Maset S, et al. (2011) DebyeHckel theory for mixtures of rigid rodlike ions and salt. *J Chem Phys* 134: 074111-1-9.
36. Bohinc K, Grime JMA, Lue L (2012) The interactions between charged colloids with rod-like counterions. *Soft matter* 8: 5679–5686.
37. Urbanija J, Bohinc K, Bellen A, et al. (2008) Attraction between negatively charged surfaces mediated by spherical counterions with quadrupolar charge distribution. *J Chem Phys* 129: 105101/1-5.

38. Ibarra-Armenta JG, Martín-Molina A, Bohinc K, et al. (2012) Effects of the internal structure of spheroidal divalent ions on the charge density profiles of the electric double layer. *J Chem Phys* 137: 224701.
39. May S, Bohinc K (2011) Attraction between like charged surfaces mediated by uniformly charged spherical colloids in a salt solution. *Croat Chem Acta* 84: 251–257.
40. Bohinc K, Reščič J, Dufreche JF, et al. (2013) Recycling of uranyl from contaminated water. *J Phys Chem B* 117: 10846–10851 251–257.
41. Gosule LC, Shellman JA (1976) Compact form of DNA induced by spermidine. *Nature* 259: 333–335.
42. Lerman LS (1971) A transition to a compact form of DNA in polymer solutions. *PNAS USA* 78: 1886–1890.
43. Jary D, Sikorav JL (1999) Cyclization of globular DNA. Implications for DNA-DNA interactions in vivo. *Biochemistry* 38: 3223–3227.
44. Vijayanathan V, Thomas T, Shirahata A, et al. (2001) DNA condensation by polyamines: a laser light scattering study of structural effects. Cyclization of globular DNA. Implications for DNA-DNA interactions in vivo. *Biochemistry* 40: 13644–13651.
45. Slita AV, Kasyanenko NA, Nazarova OV, et al. (2007) DNA-polycation complexes: Effect of polycation structure on physico-chemical and biological properties. *J Biotechnol* 127: 679–693.
46. Slonitskii SV, Kuptsov V (1989) Binding of polyamines by the double-helical DNA molecule in unfolded and compact forms. *Mol Biol (Mosk)* 23: 507–517.
47. Parsegian VA, Rand RP, Rau DC (2000) Osmotic stress, crowding, preferential hydration, and binding: A comparison of perspectives. *Proc Natl Acad Sci U S A* 97: 3987–3992.
48. Strey HH, Podgornik R, Rau DC, et al. (1998) DNA-DNA interactions. *Curr Opin Struct Biol* 8: 309–313.
49. Marty R, N'soukpoe-Kossi CN, Charbonneau D, et al. (2009) Structural analysis of DNA complexation with cationic lipids. *Nucl Acids Res* 37: 849–857.
50. Hud NV, Vilfan ID (2005) Toroidal DNA condensates: unraveling the fine structure and the role of nucleation in determining size. *Annu Rev Biophys Biomol Struct* 34: 295–318.
51. Hansma HG, Kasuya K, Oroudjev E (2004) Atomic force microscopy imaging and pulling of nucleic acids. *Curr Opin Struct Biol* 14: 380.
52. Keyser UF, van Dorp S, Lemay SG (2010) Tether forces in DNA electrophoresis. *Chem Soc Rev* 39: 939–47.
53. Baumann CG, Bloomfield VA, Smith SB, et al. (2000) Stretching of single collapsed DNA molecules. *Biophys J* 78: 1965–1978.
54. Besteman K, Van Eijk K, Lemay SG (2007) Charge inversion accompanies DNA condensation by multivalent ions. *Nat Phys* 3: 641–644.
55. Chien FT, Lin SG, Lai PY, et al. (2007) Observation of two forms of conformations in the reentrant condensation of DNA. *Phys Rev E Stat Nonlin Soft Matter Phys* 75: 041922.

56. Todd BA, Parsegian VA, Shirahata A, et al. (2008) Attractive forces between cation condensed DNA double helices. *Biophys J* 94: 4775–4782.
57. Bohinc K, Reščič J, Dufreche JF, et al. (2013) Recycling of Uranyl from Contaminated Water. *J Phys Chem B* 117: 10846–10851.
58. Bohinc K, Lue L (2011) Interaction of similarly charged surfaces mediated by nanoparticles. *Chin J Polymer Sci* 29: 414–420.
59. Grosberg AY, Nguyen TT, Shklovskii BI (2002) Colloquium: The physics of charge inversion in chemical and biological systems. *Rev Mod Phys* 74:329–345.
60. Cherstvy AG, Teif V (2013) Structure-driven homology pairing of chromatin fibers: The role of electrostatics and protein bridging. *J Biol Phys* 39: 363–385.
61. Cherstvy AG, Teif V (2014) Electrostatic effect of H1-histone protein binding on nucleosome repeat length. *Phys Biol* 11: 044001.



©2016, Klemen Bohinc, et al., licensee AIMS Press.
This is an open access article distributed under the
terms of the Creative Commons Attribution License
(<http://creativecommons.org/licenses/by/4.0>)